Chin. J. Astron. Astrophys. Vol. 8 (2008), **Supplement**, 265–272
(*http://www.chjaa.org*)

Chinese Journal of
Astronomy and
Astrophysics

Black Holes Advective Accretion Disks

G. S. Bisnovatyi-Kogan[1,2 ⋆], Yu. V. Artemova[1], I. V. Igumenshchev[3] and I. D. Novikov[4]

[1] Space Research Institute Rus. Acad. Sci, Moscow, Russia
[2] Joint Inst. Nuclear Research, Dubna, Russia
[3] Laboratory for Laser Energetics, Univ. of Rochester, NY, USA
[4] Astro-Space Center, Lebedev Phys. Inst., Moscow, Russia

Abstract We consider the effects of advection, radial gradients of pressure and radial drift velocity on the structure of accretion disks around black holes. Models with large accretion rate are investigated, where there is no continuous local solution. Continuous solutions for advective disks exist for all accretion rates. Despite the importance of advection on it's structure, the disk remains geometrically thin.

Key words: accretion disks: advection: radiative transfer

1 INTRODUCTION

The 'standard' model of accretion disk around black holes (Shakura & Sunyaev 1973) is based on a number of simplifying assumptions. In particular, it is assumed that an accretion flow has a small radial velocity, small geometrical and large optical thicknesses, and rotates with a nearly Keplerian angular velocity. These assumptions allow to neglect the radial gradient terms in the vertically averaged differential equations, reducing these equations to a set of algebraic equations. For the optically thick and low accretion rate disk with luminosity $L \ll L_{\rm Edd}$, these assumptions are generally considered to be reasonable.

It was realized, however, that the inward advection of the heat, neglected in the standard model, becomes important at higher accretion rates. The advection can crucially modify the properties of the innermost parts of the disk - the disk becomes hotter and thicker, and its rotation laws deviate from the Keplerian one. Initial attempts to solve the problem included only the effects of heat advection and radial pressure gradient in models with small values of the viscosity parameter, $\alpha = 10^{-3}$ (Paczyński & Bisnovatyi-Kogan 1981). Extensive investigation of optically thick accretion disk models with advection for a wide range of the parameters $\dot{M}$ and α was done by (Abramowicz et al. 1988). The local disk structure equations without the advection terms give rise to two branches of solutions, optically thick and optically thin, which do not intersect if $\dot{m} < \dot{m}_{\rm cr}$ (Artemova et al. 1996). For larger accretion rates there are no solutions of these equations extending continuously from large to small radii. It was argued by (Artemova et al. 1996) that for the accretion rates larger than $\dot{m}_{\rm cr}$ advection becomes critically important and would allow to exist global solutions also for $\dot{m} > \dot{m}_{\rm cr}$. Transonic solutions had been constructed by (Artemova et al. 2001) for the optically thick advective accretion disks. For some choices of $\dot{M}$ and α the latter solutions were not consistent in that respect that the effective optical depths was less than unity in the inner disk regions. This effect leads to violation of the optically thick disk approximation used by (Artemova et al. 2001) and can result in significant changes in the structure of the inner regions. In the paper by (Artemova et al. 2006) the solutions for advective accretion disks with arbitrary optical depth have been obtained, which are described below.

2 BASIC EQUATIONS

We consider equations describing the one-dimensional, height-averaged stationary accretion disk model. These equations account for the effect of advection and are adopted for the general case of the disk vertical

⋆ E-mail: gkogan@iki.rssi.ru

optical depth, with smooth transition between optically thin and optically thick accretion regimes. Here are the mass conservation equation,

$$\dot{M} = 4\pi r h \rho v, \tag{1}$$

the radial and angular momentum equations,

$$v\frac{dv}{dr} = -\frac{1}{\rho}\frac{dP_{\rm tot}}{dr} + (\Omega^2 - \Omega_K^2)r, \quad \frac{\dot{M}}{2\pi}(l - l_{\rm in}) = 2hr^2 t_{r\phi}, \tag{2}$$

and the energy equation,

$$Q_{\rm adv} = Q^+ - Q^-, \quad Q_{\rm adv} = -\frac{\dot{M}}{4\pi r}\left[\frac{dE}{dr} + P_{\rm tot}\frac{d}{dr}\left(\frac{1}{\rho}\right)\right], \tag{3}$$

$$Q^+ = -\frac{\dot{M}}{4\pi} r\Omega \frac{d\Omega}{dr}\left(1 - \frac{l_{\rm in}}{l}\right), \quad Q^- = \frac{2aT^4 c}{3\tau_0}\left(1 + \frac{4}{3\tau_0} + \frac{2}{3\tau_*^2}\right)^{-1},$$

which include the heat advection, viscous dissipation, and radiative cooling rates for arbitrary vertical optical depth, with the radiation pressure as (Artemova et al. 1996)

$$P_{\rm rad} = \frac{aT^4}{3}\left(1 + \frac{4}{3\tau_0}\right)\left(1 + \frac{4}{3\tau_0} + \frac{2}{3\tau_*^2}\right)^{-1}, \; P_{\rm tot} = P_{\rm gas} + P_{\rm rad}, \; P_{\rm gas} = \rho \mathcal{R} T. \tag{4}$$

Different optical depths are connected with scattering τ_0, by Thomson opacity κ, bremsstrahlung absorption τ_α, and effective optical depth τ_*

$$\tau_0 = \kappa\rho h, \quad \tau_\alpha \simeq 5.2 \cdot 10^{21}\frac{\rho^2 T^{1/2} h}{acT^4}, \quad \tau_* = \sqrt{\tau_\alpha(\tau_0 + \tau_\alpha)}. \tag{5}$$

Here $\Omega_K = \sqrt{GM/r(r-2r_g)^2}$ is the Keplerian angular velocity in framework of the potential $\varphi_g = GM/(r - r_g)$ (Paczyński & Wiita 1980), $2r_g = 2GM/c^2$, $\ell = \Omega r^2$, $\ell_{\rm in}$ is a constant defined by the global solution, $h = c_s/\Omega_K$ is the disk half-thickness, and $c_s = \sqrt{P_{\rm tot}/\rho}$. Viscous stress tensor was used in the form $t_{r\phi} = \alpha P_{\rm tot}$ (Shakura & Sunyaev 1973). The system of Equations (1–3) is reduced to the system of two ordinary differential equations,

$$r\frac{v'}{v} = \frac{N}{D}, \qquad r\frac{c_s'}{c_s} = 1 + \frac{x^2}{\tilde{c}_s^2}\left(\tilde{\Omega}^2 - \frac{1}{x(x-2)^2}\right) + \frac{3x-2}{2(x-2)} - \left(\frac{\tilde{v}^2}{\tilde{c}_s^2} - 1\right)\frac{N}{D}, \tag{6}$$

where N and D denote algebraical expressions, depending only on r, v, c_s, and $\ell_{\rm in}$. Explicit forms of N and D are given by (Artemova et al. 2006). The physical solution pass the singular points of Equation (6), defined by conditions $D|_{r=r_s} = 0, N|_{r=r_s} = 0$. There is an 'inner' singular point in the global accretion disk solutions, associated with the sonic point near the black hole last stable orbit at $6r_g$ (Paczyński & Bisnovatyi-Kogan 1981). This point can be a saddle or nodal-type point (see Fig. 1). The used form of the viscosity results in appearance of the second 'outer' singular point located in the subsonic region at $r \gg 6r_g$, which is always of a saddle type (Artemova et al. 2001). So the continuous global solution with two singular points is always unique.

3 NUMERICAL RESULTS

We look for solutions of three types of accretion disk models: (i) non-advective models with optical depth transition, (ii) advective models with optical depth transition, and (iii) advective models in the optically thick approximation. In the case of the small accretion rates, $\dot{m} \lesssim 0.1$, where $\dot{m} = \dot{M}/\dot{M}_{\rm Edd}$, $\dot{M}_{\rm Edd} = 4\pi cGM/\kappa c^2$, the models of all types are very similar at all radial distances. When increasing the accretion rates, the models of different types deviate significantly from each other at the small radial distances, whereas they remain similar at the larger radial distances. Below we present a comparable analysis of the models, focusing on the models with large accretion rates, $\dot{m} \gtrsim 10$.

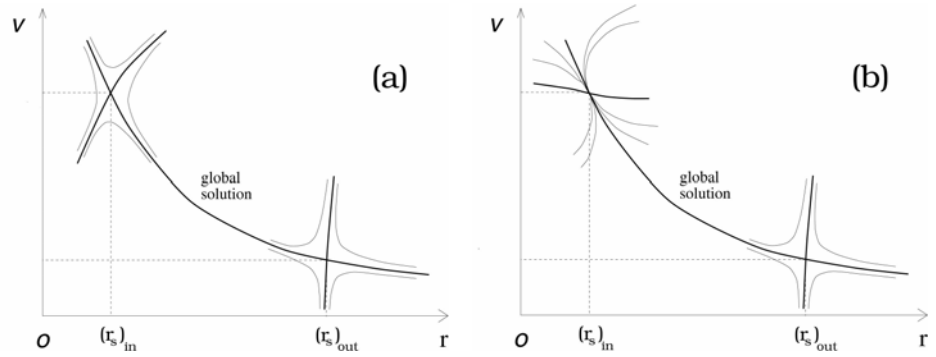

Fig. 1 Schematic illustration of behaviour of the integral curves in the vicinity of a global solution for transonic accretion disks. Two singular points exist at $r = (r_s)_{\rm in}$ and $(r_s)_{\rm out}$. The outer singular point at $(r_s)_{\rm out}$ is always of a saddle type. The inner singular point at $(r_s)_{\rm in}$ locates close to the last stable black hole orbit at $6r_g$ and changes its type from a saddle to nodal one with increase of α as shown on panels (a) and (b), respectively. Only the separatrix (thick line) which passes through both singular points represents the global solution.

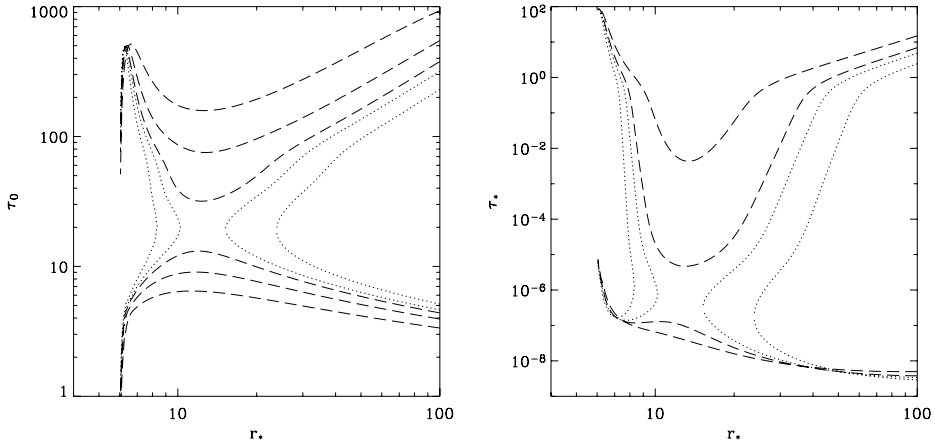

Fig. 2 Radial dependence of the Thomson scattering depth τ_0 (left panel) and the effective optical depth τ_* (right panel) for the models without advection, with $\alpha = 0.5$ and $M_{\rm BH} = 10\,M_\odot$. Dashed lines correspond to solutions with $\dot{m} < \dot{m}_{\rm cr} = 36$. The three upper lines on the left panel correspond to the optically thick family of solutions with $\dot{m} = 10, 20, 30$ (from top to bottom). The three lower lines correspond to the optically thin family of solutions with the same $\dot{m} = 10, 20, 30$ (from bottom to top). On the right panel, the two upper dashed lines correspond to the optically thick solutions with $\dot{m} = 20, 30$ (from top to bottom) and the two lower lines correspond to the optically thin solutions with $\dot{m} = 20, 30$ (from bottom to top). Dotted lines on the left and right panels correspond to the unphysical solutions with $\dot{m} = 36$ (left and right inner lines) and $\dot{m} = 50$ (left and right outer lines).

Global solutions of Equations (1–3) without the advection terms, for all radial range, exist only if the accretion rates $\dot{m} < \dot{m}_{\rm cr}$, where the critical accretion rate $\dot{m}_{\rm cr}$ depends on α and $M_{\rm BH}$. In particular, $\dot{m}_{\rm cr} = 36$ for $\alpha = 0.5$ and $M_{\rm BH} = 10\,M_\odot$; and $\dot{m}_{\rm cr} = 9$ for $\alpha = 1$ and $M_{\rm BH} = 10^8\,M_\odot$. Figure 2 shows the radial dependence of the Thomson scattering depth (left panel) and the effective optical depth (right panel) for models with $\alpha = 0.5$, $M_{\rm BH} = 10\,M_\odot$, and different $\dot{m}$.

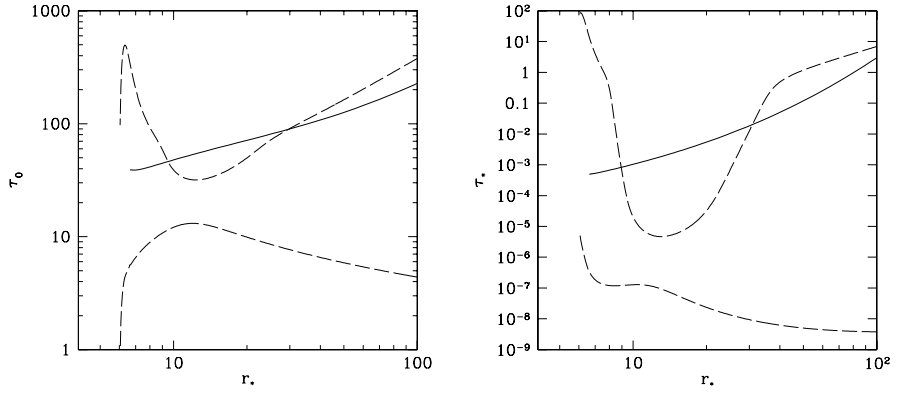

Fig. 3 Radial dependence of the Thomson scattering depth τ_0 (left) and the effective optical depth τ_* (right) for the model with $\alpha = 0.5$, $M_{\rm BH} = 10\,M_\odot$, and $\dot{m} = 30$. The dashed lines correspond to the solutions without advection. The solid lines correspond to the solution with advection and optical depth transition.

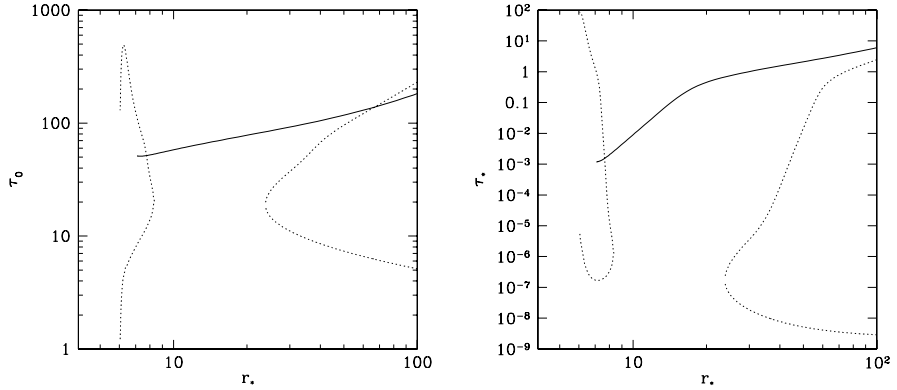

Fig. 4 Radial dependence of the Thomson scattering depth τ_0 (left) and the effective optical depth τ_* (right) for models with $\alpha = 0.5$, $M_{\rm BH} = 10\,M_\odot$, and $\dot{m} = 50$. Dotted lines correspond to the unphysical solutions without advection. The solid lines correspond to the global solution with advection and optical depth transition.

We have found solutions of Equations (1–3) with the advection terms for the optically thick family, which coincide closely with the non-advective solutions of this family at radii, $r \gtrsim 10^2 r_g$. At smaller radii, there are significant deviations between these solutions. In Figures 3 and 4, one can compare the radial profiles of τ_0 and τ_* for the advective and non-advective solutions in the case when $\dot{m}$ is close to $\dot{m}_{\rm cr}$. Figure 5 shows the radial dependence of τ_0 and τ_* (left and right panels, respectively) for the advective models with optical depth transition. The set of solutions is characterized by $\alpha = 0.5$ and $M_{\rm BH} = 10\,M_\odot$, and corresponds to $\dot{m} = 0.1$, 1, 10, 20, 30, and 50.

Figure 6 shows the radial dependence of the effective optical depth (left panel) and midplane temperature (right panel) for the advective models with and without the optical depth transition (solid and dashed lines, respectively). Note the significant increase of the temperature up to 6×10^8 K and corresponding drop of the effective optical depth down to 10^{-3} inside the radius $\sim 20 r_g$ in the model with optical depth transition. This is an illustrative example of the super-Eddington accretion, which can be discriminated in

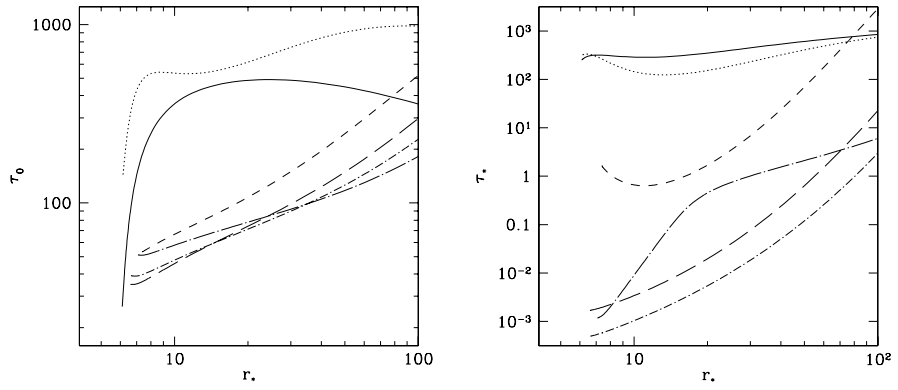

Fig. 5 Radial dependence of the Thomson scattering depth τ_0 (left) and effective optical depth τ_* (right) for models with $\alpha = 0.5$ and $M_{\rm BH} = 10\,M_\odot$. The set of solutions with advection and optical depth transition is presented for different values of accretion rates $\dot{m} = 0.1$, 1.0, 10.0, 20.0, 30.0, and 50.0 shown, respectively, by solid, dotted, dashed, long dashed, dot-dashed, and dot-long dashed lines.

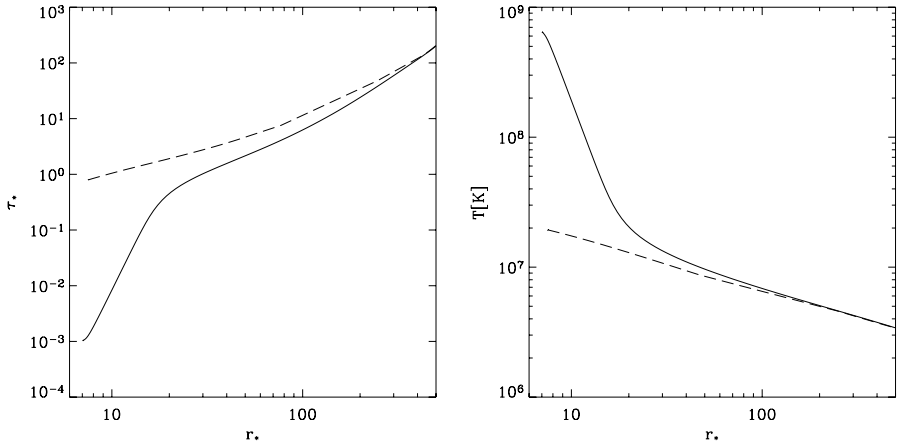

Fig. 6 Radial dependence of the effective optical depth τ_* (left) and the midplane temperature T (right) for models with $M_{\rm BH} = 10\,M_\odot$, $\alpha = 0.5$, and $\dot{m} = 48$. The dashed and solid lines correspond to the advective optically thick solution and to the advective solution with the optical depth transition, respectively.

observations due to production of soft and hard-x-rays excesses. The models with the accretion rates smaller than the critical one, $\dot{m} < \dot{m}_{\rm cr}$, do not show the prominent effectively optically thin regions and relative temperature increase. As an example, we show the model characterized by $\alpha = 0.1$, $M_{\rm BH} = 10\,M_\odot$, and $\dot{m} = 50 < \dot{m}_{\rm cr}$ with the optical depth transition (Fig. 7), in which the central temperature is increased till $T = 4 \times 10^7$ K, only by factor of 2 larger than the maximum temperature in the optically thick counterpart of this model. In the paper (Chen & Wang 2004) a unified model of accretion disks around black holes with optical depth transition was constructed. These authors considered the set of accretion disk models with $\alpha \lesssim 0.3$ and $\dot{m}$ which did not exceed $\dot{m}_{\rm cr}$. The maximum temperature in the solutions of (Chen & Wang 2004) did not exceed $T \approx 6 \times 10^7$ K, whereas our solutions show the temperatures up to 8×10^8 K in the effectively optically thin region. So, the solutions of (Chen & Wang 2004) don't differ quantitatively from the solutions obtained in the optically thick approximation.

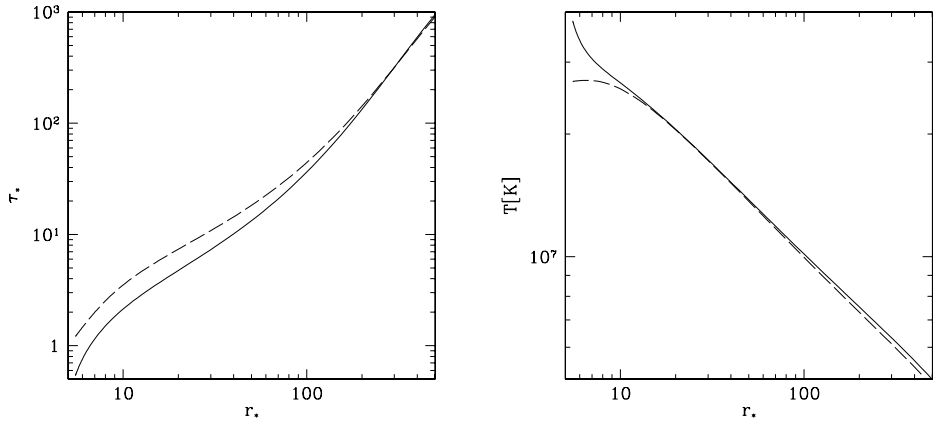

Fig. 7 Radial dependence of the effective optical depth τ_* (left) and the midplane temperature T (right) for the models with $M_{\rm BH} = 10\,M_\odot$, $\alpha = 0.1$, and $\dot{m} = 50$. Line correspondence is the same as in Fig. 6.

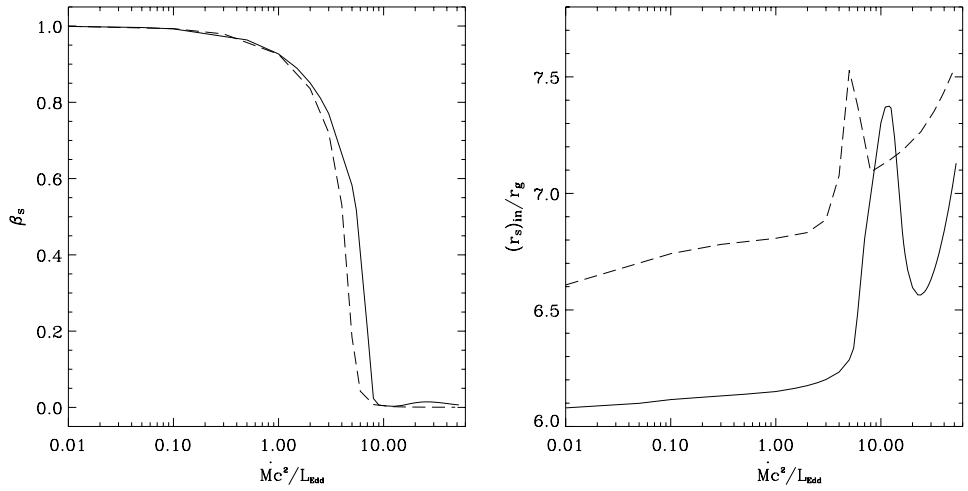

Fig. 8 Ratio of the gas pressure to total pressure β_s at the inner singular point, $(r_s)_{\rm in}$ (left panel), and position of the inner singular points $(r_s)_{\rm in}$ (right panel) as a function of the mass accretion rate $\dot{M}$ for the models with $\alpha = 0.5$ and $M_{\rm BH} = 10\,M_\odot$. Line correspondence is the same as in Fig. 6.

The difference between the advective models with and without the optical depth transition is visible in the position of the inner singular point $(r_s)_{\rm in}$, and the ratio of the gas to total pressure at this point, $\beta_s = P_{\rm g}/P_{\rm tot}$, as functions of $\dot{m}$, see Figure 8.

4 CONCLUSIONS

1. Solutions for advective disks exist for all luminosities 2. At high luminosities the solution represents disk, which is optically thick outside, and optically thin inside. 3. The temperature in the optically thin region is about a billion K, and may be responsible for appearance of hard tails.

Acknowledgements This work was partially supported by RFBR grants 05-02-17697A, 06-02-91157 and 06-02-90864. G.S.B.-K. is grateful to Franco Giovannelli and other organizers of the workshop for hospitality.

References

Abramowicz M. A., Czerny B., Lasota J. P., Szuszkiewicz E., 1988, ApJ, 332, 646
Artemova I. V., Bisnovatyi-Kogan G. S., Bjornsson G., Novikov I. D., 1996, ApJ, 456, 119
Artemova Yu. V., Bisnovatyi-Kogan G. S., Igumenshchev I. V., Novikov I. D., 2001, ApJ, 549, 1050
Artemova Yu. V., Bisnovatyi-Kogan G. S., Igumenshchev I. V., Novikov I. D., 2006, ApJ, 637, 968
Chen L.-H., Wang J.-M., 2004, ApJ, 614, 101
Paczyński B., Bisnovatyi-Kogan G. S., 1981, Acta Astr., 31, 283
Paczyński B., Wiita P. J., 1980, A&A, 88, 23
Shakura N. I., Sunyaev R. A., 1973, A&A, 24, 337
Shapiro S. L., Lightman A. P., Eardley D. M., 1976, ApJ, 204, 187

DISCUSSION

KEN EBISAWA: According to the "slim disk" model, the disk is optically thick to the last stable orbit, when the luminosity is high. Does your calculation support this idea? Can advection dominated disk be optically thick in the inner region when $L > L_{\rm Edd}$?

GENNADY BISNOVATYI-KOGAN: No. Our calculations have shown, that inner parts of the disk have effective optical depth less than unity at $\dot{m} \geq \dot{m}_{\rm cr}$, what is around $L \geq L_{\rm Edd}$. "Slim disk" model with optically thick prescription is not self-consistent at $L > L_{\rm Edd}$.

WOLFGANG KUNDT: Can you please comment on how realistic you judge the assumption of an advective flow in the disk?

GENNADY BISNOVATYI-KOGAN: Advective disk model is the only existing global model at large luminosities $L \geq L_{\rm Edd}$, in the inner parts of the accretion disk, when we consider equations averaged over the disk thickness.

ANONYMOUS REFEREE's Comment:

There is one important point in this paper which is not clear to me, and it is not clear either in the previous paper by Artemova et al. 2001. It concerns the outer boundary condition and the overall topology apart from the inner sonic point. It is clear from a number of papers that for CONSTANT ANGULAR MOMENTUM flow there are three singular points and the flow proceeds as subsonic at outer edge to supersonic close to black hole and the change subsonic/supersonic takes place EITHER at outer or at inner singular point. There is also a possibility of TWO sonic points if we consider solutions with shocks, so we then have a sequence: subsonic - supersonic - shock - subsonic - supersonic. The paper deals with angular momentum being a function of radius, but nevertheless Figure 1 is not clear. Flow starts as roughly Keplerian at the outer edge, which is clearly subsonic, so what is happening at outer sonic point? Does the flow become supersonic with respect to the local speed? If so, then why is must pass through another sonic point if it is already supersonic? How the Figure 1 would look like if the local Mach number is plotter instead of just velocity? Is the local sound speed itself equal zero somewhere?

GUENNADI BISNOVATYI-KOGAN As it is indicated in the paper (see the end of Section 2), the outer singular point is situated in the subsonic region, and does not have transonic nature. The nature of singular points in the advective disks was described by Artemova et al. (2001) for different viscosity prescriptions. The topology, shown in Figure 1 is related to αP prescription, which is used in the present calculations due to its larger numerical simplicity. This is not mathematically consistent approach, because the component $t_{r\phi}$ of the stress tensor have algebraic form, instead of differential for in the hydrodynamic Navier-Stokes equations. Appearance of the outer singular point in the subsonic region is an artifact of this approach, which nevertheless leads to quite reliable physical results. In the paper of Artemova et al. (2001) two viscosity prescriptions have been investigated. It was obtained that in the conventional differential presentation of the viscosity only ONE inner "transonic" singular point is present, while the outer one does not exist. It was shown also, that mathematical inconsistence, implied by αP viscosity have a minor influence on physical results, and both prescriptions lead to very similar results in most cases. It follows from the property, revealed by Artemova et al. (2001), that when you start integration from the outer boundary all integral curves (including the one started from the keplerian conditions) soon converge to the unique curve. This convergent curve is rather close to the Keplerian one at most part of the accretion disk, and deviations from he last one are important at approach to the last stable orbit, or to the inner singular ("sonic") point.